

This document is the unedited Author's version of a Submitted Work that was subsequently accepted for publication in the Journal of Physical Chemistry B, copyright © American Chemical Society after peer review. To access the final edited and published work see <http://pubs.acs.org/doi/abs/10.1021/jp401609p>.

Molecular Dynamics Simulation of the Arginine-Assisted Solubilization of Caffeic Acid: Intervention in the Interaction

Atsushi Hirano,^{†,‡} Tomoshi Kameda,^{‡,§} Daisuke Shinozaki,[§] Tsutomu Arakawa,^{||} and Kentaro Shiraki^{*,§}

Abstract.

We have previously demonstrated that arginine increases the solubility of aromatic compounds that have poor water solubility, an effect referred to as the “arginine-assisted solubilization system (AASS).” In the current study, we utilized a molecular dynamics simulation to examine the solubilization effects of arginine on caffeic acid, which has a tendency to aggregate in aqueous solution. Caffeic acid has a hydrophobic moiety containing a π -conjugated system that includes an aromatic ring and a hydrophilic moiety with hydroxyl groups and a carboxyl group. While its solubility increases at higher pH values due to the acquisition of a negative charge, the solubility was greatly enhanced by the addition of 1 M arginine at any pH. The results of the simulation indicated that the caffeic acid aggregates were dissociated by the arginine, which is consistent with the experimental data. The binding free energy calculation for two caffeic acid molecules in an aqueous 1 M arginine solution indicated that arginine stabilized the dissociated state due to the interaction between its guanidinium group and the π -conjugated system of the caffeic acid. The binding free energy of two caffeic acid molecules in the arginine solution exhibited a local minimum at approximately 8 Å, at which the arginine intervened between the caffeic acid molecules, causing a stabilization of the dissociated state of caffeic acid. Such stabilization by arginine likely led to the caffeic acid solubilization, as observed in both the experiment and the MD simulation. The results reported in this paper suggest that AASS can be attributed to the stabilization resulting from the intervention of arginine in the interaction between the aromatic compounds.

Key words: aromatics • drug • free energy • solubility

Introduction

Arginine has a broad application in protein research and the development of therapeutic proteins due to its suppressive effects on protein aggregation during the storage and unfolding processes. The mechanism of such arginine effects has been attributed to its interaction with the solvent-exposed hydrophobic moieties of the unfolded protein that cause protein aggregation. Some hypotheses for the origin of the arginine effect have been proposed, including the interaction of arginine with aromatic or charged residues through cation- π interactions, hydrogen bonding or salt-bridge formation,^{1,2} the gap effect using arginine

as a neutral crowder,³ and the hydrophobic interaction of arginine with the protein surface.⁴ The characteristic properties of arginine are attributed to its guanidinium group. In addition, the cluster formation of arginine in bulk solution or in the vicinity of the protein surface is considered to be partially associated with its suppressive effects on protein aggregation or stabilization by arginine.^{1,4-7} We have extended these arginine effects to small molecules to develop new applications that could enhance the solubility of drugs with low water solubility, such as drugs of type II and type IV in the biopharmaceutics classification system (BCS), which have low bioavailability *in vivo*. We also hope to further the understanding of the interaction between

[†]Nanosystem Research Institute, National Institute of Advanced Industrial Science and Technology (AIST), Tsukuba, Ibaraki 305-8562, Japan, [‡]Computational Biology Research Center (CBRC), Advanced Industrial Science and Technology (AIST), Koto, Tokyo 135-0064, Japan, [§]Institute of Applied Physics, University of Tsukuba, Tsukuba, Ibaraki 305-8573, Japan, ^{||}Alliance Protein Laboratories, San Diego, CA 92121, United States.

arginine and small molecules that have simpler structures. We have previously reported that arginine increases the solubility of some aromatic compounds (e.g., alkyl gallates, coumarin, nucleobases and acycloguanosine).⁸⁻¹⁴ In addition, other groups have reported the solubilization of naproxen by arginine.^{15,16} We have experimentally and theoretically (i.e., *via* molecular dynamics (MD) simulations) demonstrated that the solubilization mechanism is largely due to the interaction of the guanidinium group of arginine with an aromatic ring through a process known as the “arginine-assisted solubilization system” (AASS).⁸ Rajagopalan’s group has suggested that arginine behaves as a surfactant preventing the hydrophobic or aromatic interactions of organic molecules because arginine has a hydrophilic head, a hydrophobic body, and a poorly hydrated guanidinium tail above and below its plane in aqueous solution.⁷ This result is partially based on previous computational results using MD simulations to study guanidine, which were obtained by Mason *et al.*¹⁷ Rajagopalan’s group also investigated the solubilization of an aromatic peptide by arginine and attributed the solubilization mechanism to the interaction between the guanidinium group of arginine and the aromatic moieties.¹⁸

Despite the aforementioned reports, the understanding of the interaction between aromatic compounds and arginine is incomplete on the molecular level. Our objective is to further elucidate the behavior of arginine upon interaction with small aromatic compounds using MD simulations. Most of the MD simulations of arginine’s effects have been attempted to clarify the radial distribution function or the preferential interactions.^{7,18} However, the binding free energy between the solute molecules solubilized by arginine should also be considered as a key factor for AASS because the solubility of the solutes is essentially determined at equilibrium and is described by thermodynamics. Therefore, we calculated the binding free energy of two caffeic acid molecules, as a model compound, in an arginine solution. The binding free energy combined with the distribution data of arginine at each distance between the caffeic acid molecules provides new insight into the stabilization of the dissociated caffeic acid molecules in solution. Specifically, the insertion of arginine into the space between the caffeic acids accounts for the stabilization of the dissociated state of the caffeic acid. Therefore, this intervention produces the solubilization effect in the AASS. Caffeic acid is generally found in plants and beverages such as wine and coffee and is known as an active antioxidant;¹⁹ however, its poor aqueous solubility limits its practical application. Therefore, this solubilizing technique involving arginine is useful for future applications of caffeic acid in the food industry.

Experimental Section

Solubility Measurements. Caffeic acid (> 98.0%) was

obtained from Sigma-Aldrich (St. Louis, MO, USA). The L-(+)-arginine hydrochloride, sodium dihydrogenphosphate, citric acid, hydrochloric acid, and sodium hydroxide were purchased from Wako Pure Chemical Industries, Ltd. (Osaka, Japan). The caffeic acid was transferred into test tubes containing a 0 or 1 M arginine solution at various pH values, which were adjusted using hydrochloric acid or sodium hydroxide. The suspension was maintained at 40°C for 1 hour with frequent vortex mixing to dissolve the caffeic acid powders. Then, the solution was incubated at 25°C over 18 hours with frequent vortex mixing. The suspension was centrifuged at 25°C and 16,400 *xg* for 20 min to obtain supernatants saturated with caffeic acid. After either a 50-fold (for the additive-free samples) or 200-fold dilution (for samples in 1 M arginine) with a 50 mM citrate-phosphate buffer (pH 6.5), the absorbance of the supernatants was determined at 286 nm using a UV-vis spectrophotometer (ND-1000; NanoDrop Technologies, Inc.; Wilmington, DE, USA). The absorbance was converted to concentration based on the standard curve determined for caffeic acid. The solubility was determined as the average of three experiments.

Calculation of the Transfer Free Energy. The transfer free energy of the protonated caffeic acid from the additive-free solutions to the 1 M arginine solutions was calculated according to the following equation:⁸

$$\Delta G_r = \mu_a^0 - \mu_w^0 = -RT \ln(x_a / x_w) \quad (1)$$

in which

$$\begin{cases} \mu_w^0 = \mu_w - RT \ln x_w \\ \mu_a^0 = \mu_a - RT \ln x_a \end{cases}, \quad (2)$$

$$\begin{cases} x_w = n_{HA,w} / (n_{HA,w} + n_{H_2O,w}) \\ x_a = n_{HA,a} / (n_{HA,a} + n_{H_2O,a} + 2n_{a,a}) \end{cases}. \quad (3)$$

In these equations, μ_a^0 and μ_w^0 are the corresponding standard chemical potentials of the protonated caffeic acid in the presence and absence of 1 M arginine, respectively; μ_a and μ_w are the chemical potentials of caffeic acid in the presence and absence of 1 M arginine, respectively; x_a and x_w represent the corresponding mole fraction of the protonated caffeic acid in the presence and absence of 1 M arginine, respectively. In addition, $n_{i,a}$ and $n_{i,w}$ are the molarities of component *i* at saturation, and the subscripts *HA*, *H₂O*, and *a* correspond to subscript *i* and denote the protonated caffeic acid, water (additive-free solution), and arginine, respectively, in the presence and absence of 1 M arginine. In the above equations, *R* and *T* represent the gas constant and absolute temperature, respectively. The activity coefficient is considered close to unity due to the low solubility of caffeic acid.

Computational Section

Molecular Dynamics Simulation for Protonated and Deprotonated Caffeic Acid. The microscopic states of the protonated and deprotonated caffeic acid were studied in a water box using MD simulations. The calculations were performed twice for the protonated caffeic acid system and once for the deprotonated caffeic acid system. The system contained 27 caffeic acid and 13,255 water molecules, which corresponded to approximately 0.261 M caffeic acid. The caffeic acid molecules were described using the general AMBER force field (GAFF).²⁰ The water molecules were described using the TIP3P model.²¹ An restrained electrostatic potential (RESP) charge was used for the caffeic acids.²² The simulations were conducted with the NPT ensemble (300 K, 1 bar) in a rectangular box with dimensions of approximately 83.7 Å (x-axis), 78.2 Å (y-axis), and 72.4 Å (z-axis). The temperature was controlled using a Langevin thermostat with a viscosity of 0.5 ps⁻¹. The pressure was controlled by a Berendsen barostat²³ with relaxation times of 2.0 ps. The electrostatics were treated using the particle mesh Ewald (PME) method²⁴ with a 10.0-Å cutoff distance. The van der Waals interactions were expressed using the twin-range cutoff method with 10.0- and 12.0-Å cutoff distances. The covalent bonds for the hydrogen atoms in caffeic acid were constrained using the linear constraint solver (LINCS).²⁵ The covalent bonds in the water were constrained using the SETTLE algorithm. The integration time step was 2 fs. The simulations were conducted using the GROMACS 4.5.5 simulator.²⁶

Free Energy Calculation for the Interaction between Protonated Caffeic Acids in Water and Arginine Solutions. The thermodynamic interaction between two protonated caffeic acids in the presence and absence of 1 M arginine was investigated using MD simulations. The arginine molecules were described using the AMBER99SB force field.²⁷ We performed an umbrella sampling simulation to determine the free energy profile of the system, which had been previously performed.⁸ In umbrella sampling, the change in the free energy, $A(\xi)$, along the order parameter ξ is acquired by combining the potential mean force (PMF) along ξ using an MD or Monte Carlo simulation. These simulations are performed with a series of bias potentials for efficient sampling over the entire range of the order parameter. The relevant range of the order parameter is divided into bins. Then, each bias potential, $w_i(\xi)$, is assigned to a window. The simulation produces the PMF of the biased system as follows:

$$A_i^b(\xi) = -\frac{1}{\beta} \ln P_i^b(\xi) \quad (4)$$

in which $\beta = 1/k_B T$. The PME of an unbiased system in each window is

$$A_i^u(\xi) = -\frac{1}{\beta} \ln P_i^b(\xi) - w_i(\xi) + F_i \quad (5)$$

in which F_i is a constant.

The weighted histogram analysis method (WHAM) is the most popular method for combining PMFs of a biased system.²⁸ The umbrella integration (UI), as used in this study, has been further developed for WHAM with some advantages.^{29,30} Each bin of the UI is calculated from the derivative of the unbiased PME as shown in the following equation:

$$\frac{\partial A_i^u(\xi)}{\partial \xi} = -\frac{1}{\beta} \frac{\partial \ln P_i^b(\xi)}{\partial \xi} - \frac{dw_i(\xi)}{d\xi} \quad (6)$$

Kästner and Thiel demonstrated that if the restraint potential has a harmonic formula, then

$$w_i(\xi) = \frac{1}{2} K (\xi - \xi_i^c)^2 \quad (7)$$

in which ξ_i^c is the center of the window and $P_i^b(\xi)$ is well approximated by a normal distribution. Therefore, equation 6 can be rewritten as follows:

$$\frac{\partial A_i^u(\xi)}{\partial \xi} = -\frac{1}{\beta} \frac{\xi - \bar{\xi}_i^b}{(\sigma_i^b)^2} - K(\xi - \xi_i^c) \quad (8)$$

in which $\bar{\xi}_i^b$ is the mean of the biased simulation in the window i and σ_i^b is the variance.

For this study, we defined the order parameter ξ as the distance between the center of mass for the protonated caffeic acids. The umbrella sampling was conducted for $\xi = 3.0$ – 14.5 Å, which was divided into 24 bins with window lengths of 0.5 Å. Using $K \approx 239$ kcal/mol/Å² (≈ 1000 kJ/mol/Å²), 10-ns MD simulations were performed in each window in which the last 9 ns of data were analyzed and used to determine the free energy. The total simulation time was 1920 ns.

The biased simulation procedure was nearly identical to that of the previously described MD simulation of 27 caffeic acid molecules. The atomic coordinates of the amino acids were described by an AMBER ff99SB force field.²⁷ The charges on the side chains were assigned based on neutral pH conditions. The system contained 1620 water molecules and 40 chloride ions, which were added to neutralize the net charge. The molecules were placed in a dodecahedron box with 45-Å sides. Fujitani *et al.* previously utilized AMBER ff99 and GAFF with AM1-BCC charges, similar to our system, to predict the binding affinity between a protein and small compounds and obtained calculated and experimental data that were in good agreement.³¹ Therefore, we concluded that this force field was suitable for use in our MD simulations of the interaction between two protonated

caffeic acids. However, to the best of our knowledge, there is no published experimental data such as the solvation free energy.

Principal component analysis (PCA) was employed to analyze the free energy landscape.³²⁻³⁴ First, we selected 612,000 configurations of the protonated caffeic acid from a snapshot of the last 9 ns of the simulation at $\xi = 4.0\text{--}12.0$ Å in water and in a 1 M arginine solution. We considered the common region of the system in which all heavy atoms of the protonated caffeic acid and arginine were used for PCA. These conformations were superimposed onto a reference conformation, and the caffeic acid positions were fitted to those of the caffeic acid in the reference conformation. Then, the variance-covariance matrix of the ensemble was diagonalized to obtain the eigenvectors (PC axes) and eigenvalues (λ_i) (the standard deviations of the conformational distribution along the i th PC axis). Here, $\lambda_i / \sum_i \lambda_i$ was regarded as the relative contribution of the distribution along the i th PC.

Result and Discussion

Because caffeic acid contains a carboxyl group, its solubility is pH dependent. Therefore, the solubilization effect of arginine should be experimentally examined at different pH values and calculated for the protonated and deprotonated forms using MD simulations. We first present the experimental results of caffeic acid solubility in the presence and absence of arginine over a pH range of approximately 3.5–5.5 and then demonstrate the molecular mechanism for the solubilization of each form of caffeic acid using MD simulations. The solubility data yielded the transfer free energy, which describes the thermodynamic stabilization of caffeic acid when it is transferred from an additive-free solution to an arginine solution. The MD simulation provides the interaction mechanism between the arginine and the caffeic acid and its thermodynamic effects on the interactions between the caffeic acid molecules. These results, which are subsequently discussed, should aid in understanding the effects of arginine on the solubilization.

Solubility Experiment. The aqueous solubility was determined as the concentration of a compound in a saturated solution containing excess solid. By assuming that the deprotonated form is fully soluble in aqueous solution, the intrinsic solubility (S_0) of the protonated form can be calculated by fitting the following

equation to the data:

$$\begin{aligned} S &= S_0 \left(1 + \frac{K_a}{[H^+]} \right) \\ &= S_0 (1 + 10^{\text{pH} - \text{p}K_a})^2 \end{aligned} \quad (9)$$

in which S denotes the apparent solubility of the caffeic acid (i.e., the sum of the solubility of the protonated and deprotonated forms) measured directly in the solubility experiment, and the $\text{p}K_a$ is the acid dissociation constant for caffeic acid. Equation 9 indicates that the apparent solubility of caffeic acid in an aqueous solution is dominated by the pH of the solution.

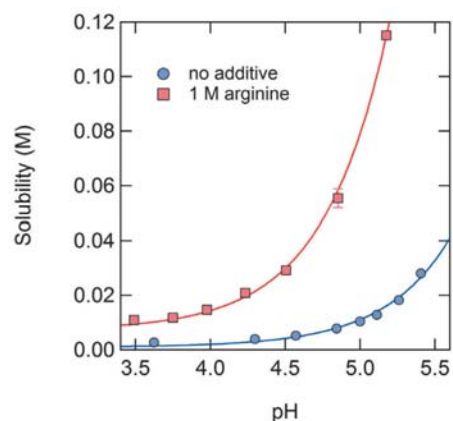


Figure 1. Solubility of caffeic acid in an additive-free solution (circles) or a 1 M arginine solution (squares).

Figure 1 shows the experimental results of the apparent solubility of caffeic acid in the presence and absence of 1 M arginine. The apparent solubility (S) increased with increasing pH in both the additive-free and 1 M arginine solutions and was greater in the 1 M arginine solution regardless of pH. By fitting equation 9 to the data, the intrinsic solubility of the protonated form (S_0) in the additive-free solution was determined to be ~ 1.2 mM. In addition, the $\text{p}K_a$ of caffeic acid in the additive-free solution was found to be ~ 4.1 . Assuming that the $\text{p}K_a$ of the carboxyl group in caffeic acid is not altered by the arginine, the fitting indicates that the intrinsic solubility was enhanced by 1 M arginine to be ~ 8.9 mM. The ratio of the apparent solubility in the additive-free solution to that in the 1 M arginine solution was found to be ~ 7 in the pH range examined in this study.

Table 1. Transfer free energy of various aromatics from an additive-free solution to a 1 M arginine solution.

Compound	Transfer free energy (kJ/mol)	Reference
Caffeic acid	-5 kJ/mol	This paper
Alkyl gallates ^a	-3 kJ/mol	8
Coumarin	-2 kJ/mol ^c	9
Tyrosine ^c	-1 kJ/mol ^c	49
Phenylalanine ^c	-0.5 kJ/mol ^c	49
Nucleobases ^b	-1--2 kJ/mol	10

^a Methyl, ethyl, propyl and butyl gallate. ^b Adenine, guanine, cytosine, thymine and uracil at pH 7.4. ^c The transfer free energy was roughly calculated by $\Delta G_{tr} \approx -RT \ln (S/S_w)$ in which ΔG_{tr} is the transfer free energy of the amino acid from the additive-free solution to the solution with the additive, R is the universal gas constant, T is the absolute temperature, and S and S_w are the solubility in a 1 M arginine solution and water (or additive-free solution), respectively.

Transfer Energy from the Additive-Free Solution to the Arginine Solution. The transfer free energy of caffeic acid from the additive-free solution to the 1 M arginine solution was calculated from the solubility data using equation 1 and assuming that the chemical potential of the solid phase is independent of the presence of arginine. This assumption is often made when the transfer free energy is calculated from solubility measurements.^{8,35,36} The transfer free energy was determined to be -5 kJ/mol. This transfer free energy was the highest among the low-molecular-weight compounds that either our group or other groups have tested for solubilization using arginine (Table 1). Our previous study suggested that the guanidinium group of the arginine interacts with the aromatic groups *via* cation- π or π - π interactions leading to the solubilization by arginine. Caffeic acid has a phenolic group and an acrylic group with a conjugated system of π -electrons. Therefore, a much greater potential exists for interactions between the guanidinium group of arginine and the caffeic acid, which accounts for the highest reported transfer free energy. The arginine may have a much greater solubilizing effect on compounds with larger π -conjugated systems. As shown Table 1, the transfer free energy of tyrosine is more negative than that of phenylalanine, which suggests that the phenol group is stabilized more by arginine than the phenyl group. The larger transfer free energy of caffeic acid may also be attributed to the phenol group.

Molecular Dynamics Simulation of Caffeic Acid Solubilization in an Arginine Solution. Computational studies are useful for understanding the behavior of arginine in the solubilization process. We report the results from an MD simulation of caffeic

acid solubilization in the presence of arginine. First, a molecular dynamics simulation of 27 protonated (uncharged) caffeic acid molecules in water (261 mM) was calculated in a cubic box with an NPT ensemble ($P = 1$ bar). The concentration was ~200-fold higher than the intrinsic solubility (S_0) of caffeic acid as determined by the experiment. Figure 2A provides representative snapshots of the simulation. The caffeic acid molecules, which were initially located in a lattice pattern at 0 ns, began to aggregate after 1 ns and clumped into a large aggregate after 33 ns (see Supporting Information, Movie S1). An additional simulation was performed to confirm the reproducibility of the simulation and led to an essentially identical result as indicated in Figure 2A. In contrast, the deprotonated (charged) caffeic acid molecules did not form large aggregates except for the occasional formation of small oligomers, which was attributed to the electrostatic repulsion between the carboxyl groups (see Supporting Information, Movie S2). Next, the protonated caffeic acid aggregate was transferred to a 1 M arginine solution as shown at 0 ns in Figure 2B. Disaggregation of the aggregate into smaller oligomers and solubilization into monomeric caffeic acid molecules occurred at 25 ns followed by a further dispersion at 50 ns. Complete disaggregation occurred at approximately 118 ns (see Supporting Information, Movie S3). Therefore, the effect of arginine on the solubilization of caffeic acid was demonstrated *in silico*. To the best of our knowledge, this is the first report of a study in which MD simulations were used to predict the aggregation and solubilization of low-molecular-weight compounds with arginine.

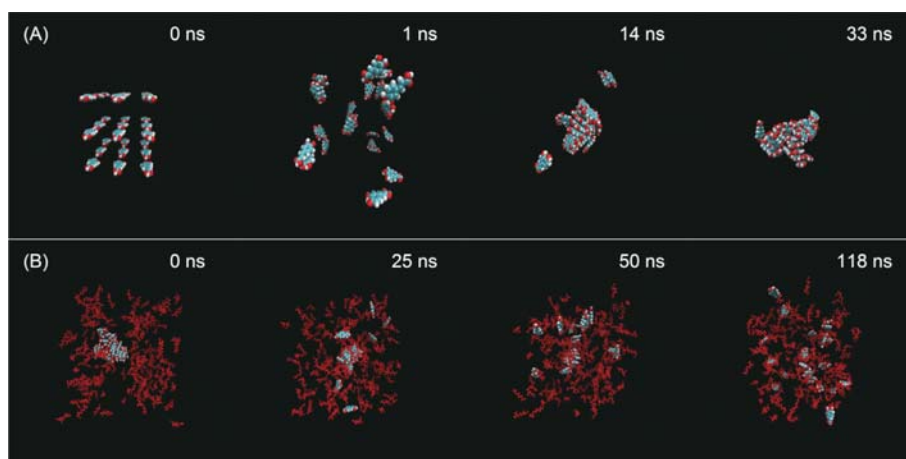


Figure 2. Snapshot of the aggregation reaction of 27 caffeic acid molecules in water (A) and the solubilization of the aggregate in 1 M arginine solution (B) at each time calculated by an MD simulation. The caffeic acid and arginine structures are represented by spheres and sticks, respectively.

Binding Free Energy Profile of Two Caffeic Acid Molecules.

A thermodynamic study of the interaction between caffeic acid molecules aids in elucidating the molecular mechanism for solubilization because the solubility is determined at equilibrium and can be expressed using thermodynamic parameters as shown in Table 1. We previously reported a thermodynamic analysis using MD simulations of the interaction between arginine or lysine and alkyl gallates, which provided the binding free energy as a function of the distance between the arginine and alkyl gallates.⁸ The results suggested that arginine binds more strongly than lysine to the alkyl gallates *via* a cation- π or π - π interaction. However, the previous simulation of the interaction between one amino acid molecule and one solute with low solubility does not necessarily reflect the behavior of the solute in amino acid solutions. Therefore, we performed the first thermodynamic analyses of the interaction between two solute molecules (i.e., caffeic acid molecules) in water and in a 1 M arginine solution using MD simulations, which was expected to more accurately reflect the solubilization thermodynamics.

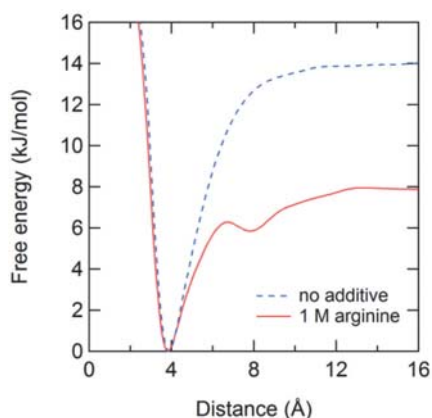


Figure 3. Binding free energy of two caffeic acid molecules in the presence (solid line) and absence (broken line) of 1 M arginine.

Protonated caffeic acid was used for the thermodynamic analyses because, as previously mentioned, the apparent solubility of caffeic acid depends on its intrinsic solubility. Figure 3 shows the binding free energy of two protonated caffeic acid molecules as a function of the distance between these two molecules. The free energy minimum occurred at approximately 4 Å in both the water and 1 M arginine solutions in which the two caffeic acid molecules were in direct contact. As the distance increased, the free energy of the state increased. At distances greater than 15 Å, the free energy plateaued indicating that the caffeic acid molecules no longer interacted with each other. The plateau value in the 1 M arginine solution was significantly lower than that in water (i.e., the former value was ~ 7.5 kJ/mol and the latter was ~ 14 kJ/mol). Therefore, the caffeic acid molecules were more weakly associated with each other in the arginine solution than in water, which suggests that the arginine stabilizes the dissociated state of the caffeic acid. More importantly, the binding free energy in the 1 M arginine solution has a local minimum at approximately 8 Å, which was not observed in water. Therefore, this unique behavior of arginine at this distance is considered important for understanding the solubilization effect of arginine.

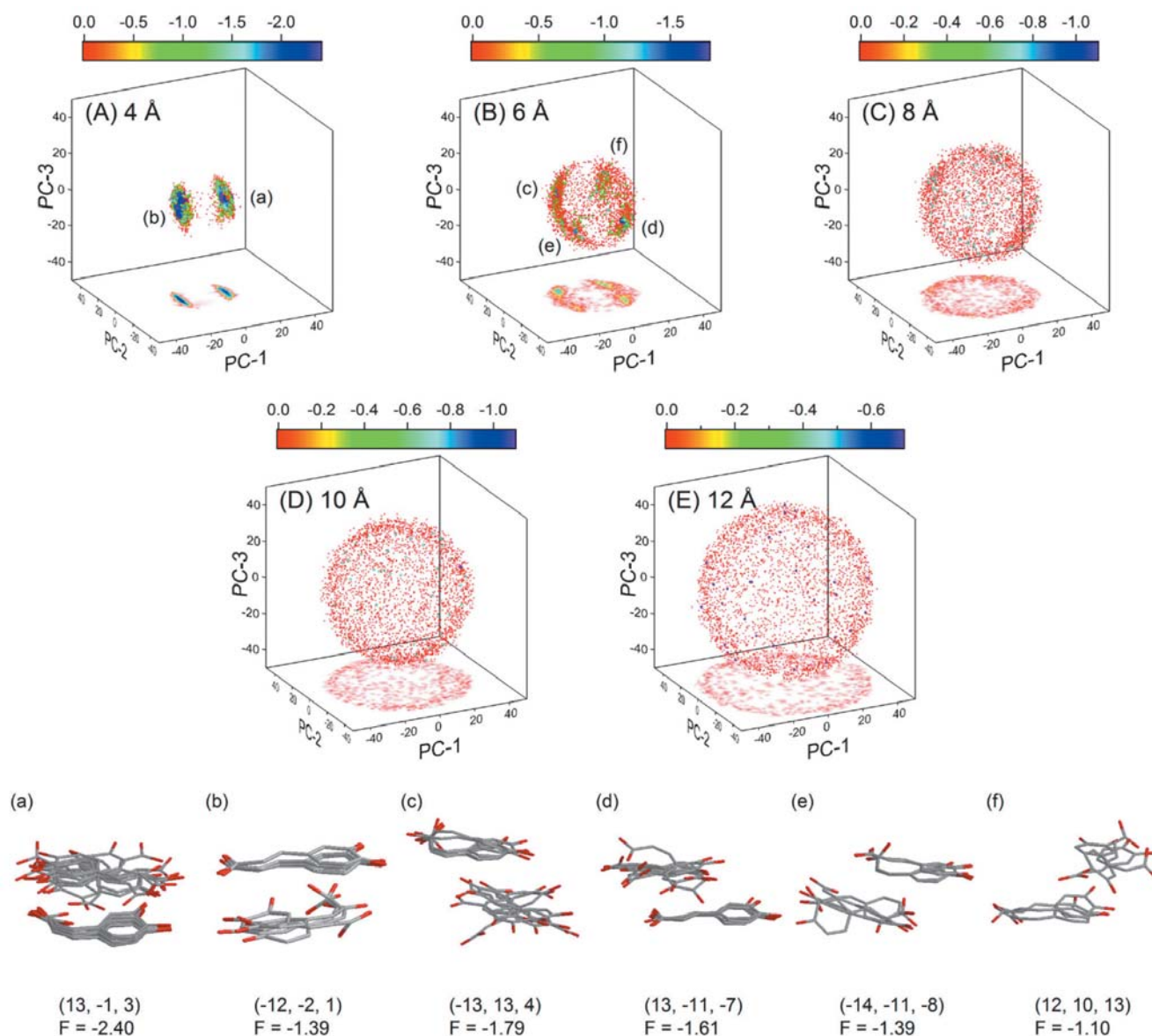


Figure 4. Three-dimensional free energy landscapes of the binding free energy of two caffeic acid molecules in water expressed along the principal component axes at each distance: (A) 4 Å (B) 6 Å (C) 8 Å (D) 10 Å (E) 12 Å. The colors of the spheres correspond to the free energy level displayed above. The bottom figures show the two-dimensional free energy landscape. The colors were arbitrarily normalized for convenience. The structures corresponding to the lowest free energy of the clusters (a)–(f) are shown in the lower models.

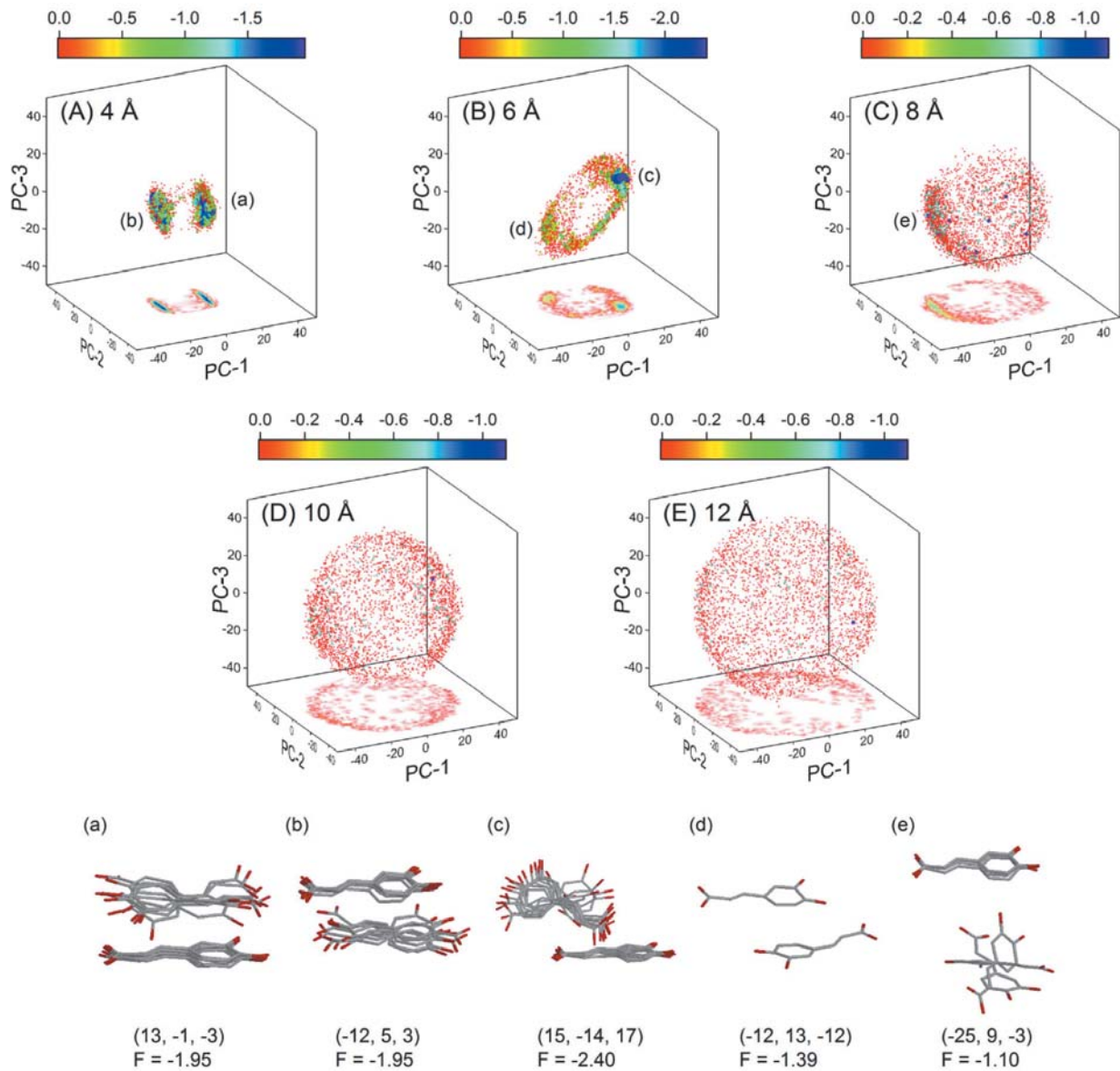


Figure 5. Three-dimensional free energy landscape of the binding free energy of two caffeic acid molecules in a 1 M arginine solution expressed along the principal component axes at each distance: (A) 4 Å (B) 6 Å (C) 8 Å (D) 10 Å (E) 12 Å. The colors of the spheres correspond to the free energy level displayed above. The bottom figures show the two-dimensional free energy landscape. The colors were arbitrarily normalized for convenience. The structures corresponding to the lowest free energy of the clusters (a)–(f) are shown in the lower models.

Principal Component Analyses of the Conformation of Two Caffeic Acid Molecules. Investigating the conformational characteristics of the solubilization system is useful in understanding the thermodynamic effects of arginine. Although caffeic acid is not a large molecule, the conformational space of the present system is too large to intuitively describe its characteristics. Therefore, we expressed the conformational space of the system with a few axes using PCA, which classifies the conformations with as few dimensions as possible. Figure 4 shows the PCA for the caffeic acid molecular conformations in water. The PCA corresponds to the three-dimensional free energy landscape at each distance between the two caffeic acid molecules in water. Similarly, Figure 5 provides the corresponding PCA for the 1 M arginine solution. The colors of the spheres displayed in these figures correspond to the free energy (see the legend above each figure). The contributions of PC-1, PC-2, and PC-3 were 34.3%, 28.1%, and 24.7%, respectively, and the total contribution of the PC was 87.2%, which is sufficient to describe the free energy landscape of the interaction between the caffeic acid molecules. Figures shown on the bottom of the three-dimensional PCA are two-dimensional free energy landscapes obtained by mapping the three-dimensional free energy landscape onto a two-dimensional PC-1–PC-2 plane. The colors of the two-dimensional free energy were arbitrarily normalized for convenience.

When the distance between the caffeic acid molecules was 4 Å, the conformation of the caffeic acid molecules in water was roughly divided into two clusters depicted in (a) and (b) (Figure 4A). Figure 4a and b show the conformations of the caffeic acid molecules that correspond to the respective minima of the free energy represented by (a) and (b) in Figure 4A. The most stable conformation (a) was located at (13, -1, 3) with $F = -2.40$. The second most stable conformation (b) was located at (-12, -2, 1) with $F = -1.39$. These figures show the aromatic rings of the caffeic acid molecules stacked together in a face-to-face conformation with either a head-to-head or head-to-tail association at 4 Å. The characteristic conformations at this distance are likely due to the steric hindrance between the caffeic acid molecules. The conformational and free energy profile of the interaction between the caffeic acid molecules changed substantially at 6 Å from that at 4 Å (Figure 4B). At this distance, there were primarily four clusters, which are depicted

by (c), (d), (e), and (f). The most stable conformations at this distance as shown in (c) were located at (-13, 13, 4) with $F = -1.79$. The value of the free energy for this cluster was significantly higher than the minimum value at 4 Å. In addition, the face-to-face stacking at 6 Å was significantly looser than that at 4 Å. As the distance between the caffeic acid molecules continued to increase, the conformational space expanded, as shown in Figure 4C–E, increasing the free energy of each cluster as the distance increased. In Figure 4C–E corresponding to 8, 10, and 12 Å, respectively, the clusters were no longer observed in the three-dimensional PC spaces.

In the 1 M arginine solution, the free energy profile of the interaction between the caffeic acid molecules differed from that in water (Figure 5A–E). The conformational profile in the arginine solution at 4 Å (Figure 5A) was nearly identical to that in water (Figure 4A) (i.e., two clusters were observed, and the caffeic acid molecules interacted with each other in a face-to-face fashion). The free energy for both primary clusters depicted in (a) and (b) was $F = -1.95$, which is considerably higher than the minimum value in water at 4 Å. Therefore, the conformational space in the arginine solution was somewhat expanded over that in water. At 6 Å (Figure 5B), the conformational and free energy profile in the arginine solution were substantially different from those obtained in water (Figure 4B). Only two clusters, which are depicted in (c) and (d), were found in the arginine solution. The most stable conformation at this distance, which is depicted in (c), was located at (15, -14, 17) with $F = -2.40$. The value of the free energy was lower than that at 4 Å, indicating that a large population was located at cluster (c) compared with the case at 4 Å even though the conformational space at 6 Å was expanded more than that at 4 Å. The free energy was not only more negative than the minimum value at 4 Å in the arginine solution but also comparable to that at 4 Å in water. Another cluster was located in an opposite position (-12, 13, -12), which is depicted in (d) with $F = -1.39$ (Figure 5B). A stable conformation, which is depicted in (e), was found at 8 Å in the arginine solution (Figure 5C), although no cluster was found at this distance in water (Figure 4C). The conformation depicted in (e) was located at (-25, 9, -3) with $F = -1.10$. Based on these results, the arginine was found to confine the interaction between caffeic acid molecules dramatically altering the conformational spaces.

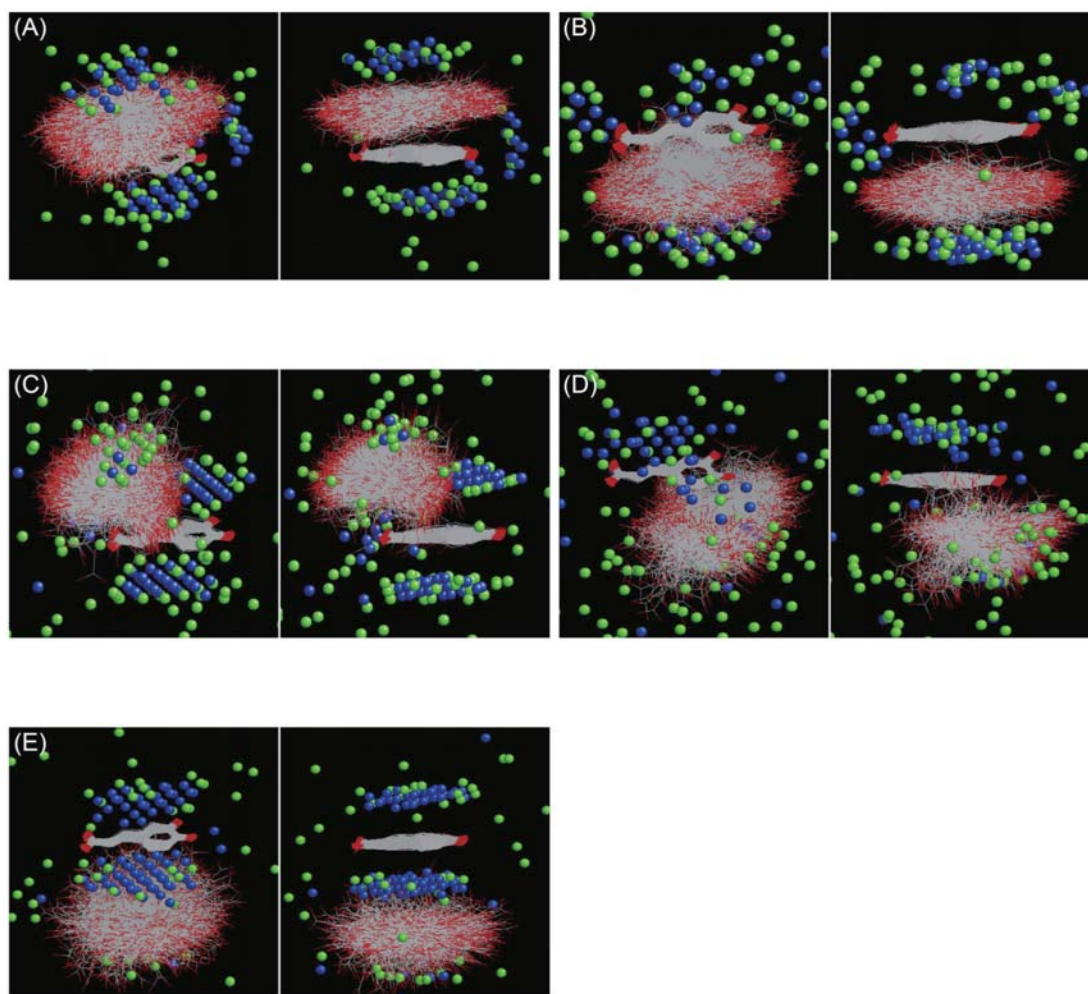


Figure 6. The population density maps of the guanidinium group of arginine around the caffeic acid molecules. Each figure (A)–(E) corresponds to the clusters (a)–(e) in Figure 5A–E. For each cluster, the two figures demonstrate from different viewpoints. The colors of the spheres correspond to the number density of the guanidinium group’s center of mass: Blue indicates a density that is more than 10 times the average value, and green indicates a density that is 7–10 times the average value. All caffeic acid conformations belonging to each cluster are merged with the maps.

Distribution Mapping of the Guanidinium Group of Arginine around the Caffeic Acid Molecules. Investigating the behavior of arginine in the interaction between the caffeic acid molecules is essential to understanding its role in the stabilization. Figure 6A–E provides the conformations of the caffeic acid molecules and the distribution of the guanidinium group of arginine that corresponds to the clusters depicted in (a)–(e) in Figure 5A–C. Each sphere indicates the position of the center of mass for the guanidinium group, and its color indicates the number density. The guanidinium group of arginine has a tendency to be near the aromatic or hydrophilic groups of caffeic acid (Figure 6A and B) at 4 Å. No guanidinium group was located between the caffeic acid molecules at this distance because the caffeic acid molecules interact closely with each other at 4 Å, as shown in Figure 5a and b. The guanidinium group of arginine reportedly has the ability to interact with

carboxyl groups *via* hydrogen bonding.^{1,37,38} Such interactions can be attributed to the distribution of the guanidinium group around the hydrophilic groups of caffeic acid although its interaction with the protonated carboxyl groups is expected to be somewhat weaker than that with the charged carboxyl groups.^{4,7} The most stable conformation at 6 Å indicated an insertion of arginine into the small space made by the two caffeic acid molecules (Figure 6C); arginine forced the conformation of the caffeic acid molecules into the intervened conformation. A minor stable conformation with a comparatively scattered distribution was also noted (Figure 6D). At 8 Å, the arginine completely intervened in the interaction between the caffeic acid molecules, as shown in Figure 6E. At this distance, the guanidinium group of arginine interacted less with the hydrophilic groups of caffeic acid. Therefore, the arginine should interact with the hydrophobic moieties or the π -conjugated system including

the aromatic group *via* the hydrophobic, π - π and cation- π interactions. Our previous study suggested that arginine interacts with aromatics *via* the π - π and cation- π interactions.⁸ In addition, Mason *et al.* indicated that guanidine is poorly hydrated above and below its plane in aqueous solutions.¹⁷ This property of the guanidinium group of arginine may be the origin of the hydrophobicity that is associated with the hydrophobic interactions.⁷ Based on these results, we have successfully demonstrated that arginine stabilizes caffeic acid molecules *via* its interaction with the hydrophobic and hydrophilic moieties at short distances (i.e., 4 or 6 Å). The arginine primarily interacts with the π -conjugated system or the hydrophobic moieties at 8 Å at which the arginine can intervene into the space between the caffeic acid molecules.

The interaction of caffeic acid with arginine observed at 8 Å is likely critical to the stabilization of caffeic acid over a wide range of distances beyond 8 Å. As previously mentioned, the significant stabilization at 8 Å was attributed to the replacement of the interactions between the caffeic acid molecules by the interactions between the caffeic acid and arginine. At distances much greater than 8 Å, the binding free energy appeared to plateau, suggesting that the intervention of arginine in the interaction between caffeic acid molecules also occurred at 8–12 Å. We concluded that the stabilization over a long distance caused by this intervention accounts for the solubilization observed in the results from both the experiments and MD simulations. This stabilization is primarily due to π - π , cation- π , or hydrophobic interactions. Rajagopalan's group reported that arginine forms a solvation layer around hydrophobic or aromatic particles at intervals of ~10 Å, leading to their solubilization.⁷ Therefore, the behavior of arginine around interfaces at subnanometer distances should be closely associated with their stabilization and solubilization.

Finally, we offer a perspective on the future challenges regarding the AASS mechanism based on the current results. While caffeic acid exhibits antioxidant activity,¹⁹ its low aqueous solubility limits its practical application in the food industry. Solubilizing caffeic acid using arginine could provide an alternative to other solubilization techniques such as physicochemical formulations and chemical modifications.^{39,40} Another potential application might involve the interaction of arginine or proteins with nanoscale particles, such as carbon nanotubes, that are often associated with cytotoxicity, therapeutic applications, or drug delivery. The interactions between an aromatic moiety and arginine described in this paper are applicable to the interfaces between nanoscale particles and their solvents. Rajagopalan's group used MD simulations to investigate the interaction between arginine and subnanoscale hydrophobic and aromatic particles that can lead to the solubilization of the particles. Our group and others have demonstrated that proteins, such as lysozyme, can be

incorporated into and disperse carbon nanotubes.^{41–47} Calvaresi *et al.* showed that the interaction between carbon nanotubes and lysozyme is primarily due to the interaction between the arginine residues of lysozyme and the carbon nanotube surfaces.⁴⁸ The AASS mechanism can also be applied to understand such interactions and should be investigated further.

Conclusion

This study demonstrated, for the first time, the solubilization dynamics of an aromatic compound (i.e., caffeic acid) by arginine. The local minimum of the binding free energy between the caffeic acid molecules at approximately 8 Å was attributed to the intervention of arginine in their interaction, which is related to the solubilization mechanism of the AASS. The driving force of the intervention is likely due to the interaction of the guanidinium group of arginine with the π -conjugated system, such as a cation- π or π - π interaction. Insight into the AASS is useful for plying arginine to the solubilization of aromatic drugs and for understanding the mechanism by which arginine can prevent protein aggregation.

ASSOCIATED CONTENT

Supporting Information. MD movies of the solubilization of caffeic acid in arginine solution. This material is available free of charge *via* the Internet at <http://pubs.acs.org>.

Corresponding Author

* E-mail: shiraki@bk.tsukuba.ac.jp. Phone: +81-29-853-5306. Fax: +81-29-853-5215.

Author Contributions

These authors contributed equally.

Notes

The authors declare no competing financial interest.

Acknowledgments

We wish to thank T. Hirakawa for scientific discussions. This work was partially supported by the Toyo Institute of Food Technology, JSPS KAKENHI Grant Numbers 23550189, 24750172 and the Platform for Drug Discovery, Informatics, and Structural Life Science from the Ministry of Education, Culture, Sports, Science and Technology, Japan. The theoretical calculations were performed using the Research Center for Computational Science, Okazaki, Japan and the supercomputing resources were provided by the Human Genome Center (Univ. of Tokyo).

REFERENCES

1. Shukla, D.; Trout, B. L. Interaction of Arginine with Proteins and the Mechanism by Which It Inhibits Aggregation. *J. Phys. Chem. B* **2010**, *114*, 13426-13438.
2. Tsumoto, K.; Umetsu, M.; Kumagai, I.; Ejima, D.; Philo, J. S.; Arakawa, T. Role of Arginine in Protein Refolding, Solubilization, and Purification. *Biotechnol. Prog.* **2004**, *20*, 1301-1308.
3. Baynes, B. M.; Trout, B. L. Rational Design of Solution Additives for the Prevention of Protein Aggregation. *Biophys. J.* **2004**, *87*, 1631-1639.
4. Das, U.; Hariprasad, G.; Ethayathulla, A. S.; Manral, P.; Das, T. K.; Pasha, S.; Mann, A.; Ganguli, M.; Verma, A. K.; Bhat, R. et al. Inhibition of Protein Aggregation: Supramolecular Assemblies of Arginine Hold the Key. *PLoS ONE* **2007**, *2*, e1176.
5. Vagenende, V.; Han, A. X.; Mueller, M.; Trout, B. L. Protein-Associated Cation Clusters in Aqueous Arginine Solutions and Their Effects on Protein Stability and Size. *ACS Chem. Biol.* **2012**, , .
6. Schneider, C. P.; Shukla, D.; Trout, B. L. Arginine and the Hofmeister Series: The Role of Ion-Ion Interactions in Protein Aggregation Suppression. *J. Phys. Chem. B* **2011**, *115*, 7447-7458.
7. Li, J.; Garg, M.; Shah, D.; Rajagopalan, R. Solubilization of Aromatic and Hydrophobic Moieties by Arginine in Aqueous Solutions. *J. Chem. Phys.* **2010**, *133*, 054902.
8. Hirano, A.; Kameda, T.; Arakawa, T.; Shiraki, K. Arginine-Assisted Solubilization System for Drug Substances: Solubility Experiment and Simulation. *J. Phys. Chem. B* **2010**, *114*, 13455-13462.
9. Hirano, A.; Arakawa, T.; Shiraki, K. Arginine Increases the Solubility of Coumarin: Comparison with Salting-In and Salting-Out Additives. *J. Biochem.* **2008**, *144*, 363-369.
10. Hirano, A.; Tokunaga, H.; Tokunaga, M.; Arakawa, T.; Shiraki, K. The Solubility of Nucleobases in Aqueous Arginine Solutions. *Arch. Biochem. Biophys.* **2010**, *497*, 90-96.
11. Shiraki, K.; Hirano, A.; Kita, Y.; Koyama, A. H.; Arakawa, T. Potential Application of Arginine in Interaction Analysis. *Drug Discov. Ther.* **2010**, *4*, 326-333.
12. Arakawa, T.; Kita, Y.; Koyama, A. H. Solubility Enhancement of Gluten and Organic Compounds by Arginine. *Int. J. Pharm.* **2008**, *355*, 220-223.
13. Arakawa, T.; Uozaki, M.; Koyama, A. H. Modulation of Small Molecule Solubility and Protein Binding by Arginine. *Mol. Med. Report.* **2010**, *3*, 833-836.
14. Ariki, R.; Hirano, A.; Arakawa, T.; Shiraki, K. Arginine Increases the Solubility of Alkyl Gallates through Interaction with the Aromatic Ring. *J. Biochem.* **2011**, *149*, 389-394.
15. Mura, P.; Bettinetti, G. P.; Cirri, M.; Maestrelli, F.; Sorrenti, M.; Catenacci, L. Solid-State Characterization and Dissolution Properties of Naproxen-Arginine-Hydroxypropyl-beta-Cyclodextrin Ternary System. *Eur. J. Pharm. Biopharm.* **2005**, *59*, 99-106.
16. Mura, P.; Maestrelli, F.; Cirri, M. Ternary Systems of Naproxen with Hydroxypropyl-beta-Cyclodextrin and Aminoacids. *Int. J. Pharm.* **2003**, *260*, 293-302.
17. Mason, P. E.; Neilson, G. W.; Enderby, J. E.; Saboungi, M. L.; Dempsey, C. E.; MacKerell, A. D. Jr; Brady, J. W. The Structure of Aqueous Guanidinium Chloride Solutions. *J. Am. Chem. Soc.* **2004**, *126*, 11462-11470.
18. Shah, D.; Li, J.; Shaikh, A. R.; Rajagopalan, R. Arginine-Aromatic Interactions and Their Effects on Arginine-Induced Solubilization of Aromatic Solutes and Suppression of Protein Aggregation. *Biotechnol. Prog.* **2012**, *28*, 223-231.
19. Gulcin, I. Antioxidant Activity of Caffeic Acid (3,4-Dihydroxycinnamic Acid). *Toxicology* **2006**, *217*, 213-220.
20. Wang, J.; Wolf, R. M.; Caldwell, J. W.; Kollman, P. A.; Case, D. A. Development and Testing of a General Amber Force Field. *J. Comput. Chem.* **2004**, *25*, 1157-1174.
21. Jorgensen, W. L.; Chandrasekhar, J.; Madura, J. D.; Impey, R. W.; Klein, M. L. Comparison of Simple Potential Functions for Simulating Liquid Water. *J. Chem. Phys.* **1983**, *79*, 926-935.
22. Bayly, C. I.; Cieplak, P.; Cornell, W. D.; Kollman, P. A. A Well-Behaved Electrostatic Potential Based Method Using Charge Restraints for Deriving. *J. Phys. Chem.* **1993**, *97*, 10269-10280.
23. Berendsen, H. J. C.; Postma, J. P. M.; van, Gunsteren W. F.; Dinola, A.; Haak, J. R. Molecular Dynamics with Coupling to an External Bath. *J. Chem. Phys.* **1984**, *81*, 3684-3690.
24. Essmann, U.; Perera, L.; Berkowitz, M. L.; Darden, T.; Lee, H.; Pedersen, L. G. A Smooth Particle Mesh Ewald Method. *J. Chem. Phys.* **1995**, *103*, 8577-8593.
25. Hess, B.; Bekker, H.; Berendsen, H. J. C.; Fraaije, J. G. E. M. LINCS: A Linear Constraint Solver for Molecular Simulations. *J. Comput. Chem.* **1997**, *18*, 1463-1472.
26. Hess, B.; Kutzner, C.; van der Spoel, D.; Lindahl, E. GROMACS 4: Algorithms for Highly Efficient, Load-Balanced, and Scalable Molecular Simulation. *J. Chem. Theory Comput.* **2008**, *4*, 435-447.
27. Hornak, V.; Abel, R.; Okur, A.; Strockbine, B.; Roitberg, A.; Simmerling, C. Comparison of Multiple Amber Force Fields and Development of Improved Protein Backbone Parameters. *Proteins* **2006**, *65*, 712-725.
28. Ferrenberg, A. M.; Swendsen, R. H. New Monte Carlo Technique for Studying Phase Transitions. *Phys. Rev. Lett.* **1988**, *61*, 2635-2638.
29. Kastner, J.; Thiel, W. Bridging The Gap Between Thermodynamic

- Integration and Umbrella Sampling Provides a Novel Analysis Method: "Umbrella Integration". *J. Chem. Phys.* **2005**, *123*, 144104.
30. Kastner, J.; Thiel, W. Analysis of the Statistical Error in Umbrella Sampling Simulations by Umbrella Integration. *J. Chem. Phys.* **2006**, *124*, 234106.
31. Fujitani, H.; Tanida, Y.; Ito, M.; Jayachandran, G.; Snow, C. D.; Shirts, M. R.; Sorin, E. J.; Pande, V. S. Direct Calculation of the Binding Free Energies of FKBP Ligands. *J. Chem. Phys.* **2005**, *123*, 084108.
32. Garcia, A. E. Large-Amplitude Nonlinear Motions in Proteins. *Phys. Rev. Lett.* **1992**, *68*, 2696-2699.
33. Kitao, A.; Hayward, S.; Go, N. Energy Landscape of a Native Protein: Jumping-Among-Minima Model. *Proteins* **1998**, *33*, 496-517.
34. Ikeda, K.; Galzitskaya, O. V.; Nakamura, H.; Higo, J. beta-Hairpins, alpha-Helices, and the Intermediates among the Secondary Structures in the Energy Landscape of a Peptide From a Distal beta-Hairpin of SH3 Domain. *J. Comput. Chem.* **2003**, *24*, 310-318.
35. Nozaki, Y.; Tanford, C. The Solubility of Amino Acids, Diglycine, and Triglycine in Aqueous Guanidine Hydrochloride Solutions. *J. Biol. Chem.* **1970**, *245*, 1648-1652.
36. Nozaki, Y.; Tanford, C. The solubility of Amino Acids and Related Compounds in Aqueous Urea Solutions. *J. Biol. Chem.* **1963**, *238*, 4074-4081.
37. Shah, D.; Shaikh, A. R.; Peng, X.; Rajagopalan, R. Effects of Arginine on Heat-Induced Aggregation of Concentrated Protein Solutions. *Biotechnol. Prog.* **2011**, *27*, 513-520.
38. Shukla, D.; Trout, B. L. Preferential Interaction Coefficients of Proteins in Aqueous Arginine Solutions and Their Molecular Origins. *J. Phys. Chem. B* **2011**, *115*, 1243-1253.
39. Coimbra, M.; Isacchi, B.; van, Bloois L.; Torano, J. S.; Ket, A.; Wu, X.; Broere, F.; Metselaar, J. M.; Rijcken, C. J.; Storm, G. et al. Improving Solubility and Chemical Stability of Natural Compounds for Medicinal Use by Incorporation into Liposomes. *Int. J. Pharm.* **2011**, *416*, 433-442.
40. Nishimura, T.; Kometani, T.; Takii, H.; Terada, Y.; Okada, S. Glucosylation of Caffeic Acid with *Bacillus Subtilis* X-23 alpha-Amylase and a Description of the Glucosides. *J. Ferment. Bioeng.* **1995**, *80*, 18-23.
41. Hirano, A.; Maeda, Y.; Yuan, X.; Ueki, R.; Miyazawa, Y.; Fujita, J.; Akasaka, T.; Shiraki, K. Controlled Dispersion and Purification of Protein-Carbon Nanotube Conjugates Using Guanidine Hydrochloride. *Chem. Eur. J.* **2010**, *16*, 12221-12228.
42. Hirano, A.; Uda, K.; Maeda, Y.; Akasaka, T.; Shiraki, K. One-Dimensional Protein-Based Nanoparticles Induce Lipid Bilayer Disruption: Carbon Nanotube Conjugates and Amyloid Fibrils. *Langmuir* **2010**, *26*, 17256-17259.
43. Nepal, D.; Geckeler, K. E. Proteins and Carbon Nanotubes: Close Encounter in Water. *Small* **2007**, *3*, 1259-1265.
44. Nepal, D.; Geckeler, K. E. pH-Sensitive Dispersion and Debundling of Single-Walled Carbon Nanotubes: Lysozyme as a Tool. *Small* **2006**, *2*, 406-412.
45. Bomboi, F.; Bonincontro, A.; La, Mesa C.; Tardani, F. Interactions between Single-Walled Carbon Nanotubes and Lysozyme. *J. Colloid Interface Sci.* **2011**, *355*, 342-347.
46. Xie, L. M.; Chou, S. G.; Pande, A.; Pande, J.; Zhang, J.; Dresselhaus, M. S.; Kong, J.; Liu, Z. F. Single-Walled Carbon Nanotubes Probing the Denaturation of Lysozyme. *J. Phys. Chem. C* **2010**, *114*, 7717-7720.
47. Asuri, P.; Bale, S. S.; Pangule, R. C.; Shah, D. A.; Kane, R. S.; Dordick, J. S. Structure, Function, and Stability of Enzymes Covalently Attached to Single-Walled Carbon Nanotubes. *Langmuir* **2007**, *23*, 12318-12321.
48. Calvaresi, M.; Hoefinger, S.; Zerbetto, F. Probing the Structure of Lysozyme-Carbon-Nanotube Hybrids with Molecular Dynamics. *Chem. Eur. J.* **2012**, *18*, 4308-4313.
49. Arakawa, T.; Ejima, D.; Tsumoto, K.; Obeyama, N.; Tanaka, Y.; Kita, Y.; Timasheff, S. N. Suppression of Protein Interactions by Arginine: A Proposed Mechanism of the Arginine Effects. *Biophys. Chem.* **2007**, *127*, 1-8.

SYNOPSIS

